Adaptive Antennas at the Mobile and Base Stations in an OFDM/TDMA System

Kai-Kit Wong, *Student Member, IEEE,* Roger S.-K. Cheng, *Member, IEEE,* Khaled Ben Letaief, *Senior Member, IEEE,* and Ross D. Murch, *Senior Member, IEEE*

***Abstract*—In recent years, several smart antenna systems have been proposed and demonstrated at the base station (BS) of wireless communications systems, and these have shown that significant system performance improvement is possible. In this paper, we consider the use of adaptive antennas at the BS and mobile stations (MS), operating jointly, in combination with orthogonal frequency-division multiplexing. The advantages of the proposed system includes reductions in average error probability and increases in capacity compared to conventional systems. Multiuser access, in space, time, and through subcarriers, is also possible and expressions for the exact joint optimal antenna weights at the BS and MS under cochannel interference conditions for fading channels are derived. To demonstrate the potential of our proposed system, analytical along with Monte Carlo simulation results are provided.**

***Index Terms*—Cochannel interference, flat and frequency-selective fading channels, orthogonal frequency-division multiplexing, smart antennas, wireless communication systems.**

I. Introduction

FUTURE wireless communications systems will need to be able to support a high level of user traffic along with a wide range of high-quality services that not only include high-quality voice but also data, facsimile, still pictures, and video. Providing these high-quality services over the harsh wireless channel with a limited spectrum implies that an increase in the capacity of current wireless systems will need to be achieved [1]–[4]. One possible approach to increase system capacity is through the use of smart or adaptive antennas [5], [6] that make use of spatial diversity to compensate for channel impairments without increasing the transmitted power or bandwidth.

With recent developments in hardware miniaturization and advances in antenna design [7], smart antennas at both the base (BS) and mobile stations (MS) have been suggested to achieve further increases in capacity as well as performance [3], [8], [9], [11]. The generalized problem of coded modulation with multiple transmit and multiple receive antennas has been addressed [3] while Raleigh and Cioffi [8] studied space-time water-filling for multipath fading, with prior knowledge of the channel. In [9], Kohno considered the maximization of signal-to noise ratio (SNR) by a joint multiple transmission and reception filters system. However, cochannel interference (CCI) has not been considered in any of these previous studies. Recent works by Lu *et al.* [10] and Wong *et al.* [11] have investigated the joint use of smart antennas at the BS and MS for performance improvement. In [10], zero-forcing based transmit antenna weights and minimum mean-square-error (MMSE) receive antenna weights are proposed for multichannel communication systems, but the subchannel gains can be arbitrarily small since the weights at the transmitter and receiver are not jointly optimized. Recently, the joint optimal antenna weights at both the BS and MS have been derived for interference-limited fading channels [11]. Nevertheless, large system complexity and/or degradation of system performance occurs in frequency-selective fading channels.

In this paper, we investigate the performance of the smart base and smart mobile (SBM) antennas discussed in [11] in conjunction with orthogonal frequency-division multiplexing (OFDM) [12], and we will refer to this combined SBM and OFDM system as SBM/OFDM. This approach utilizes the CCI rejection capability of the smart antennas and the intersymbol interference (ISI) rejection capability by OFDM. Hence, multiple users can be accessed in space, time, and by subcarriers. Therefore, one may expect that significant improvement of system performance as well as capacity is possible.

To analyze the performance of SBM/OFDM, the average bit-error rate (BER) performance of our proposed system is found by Monte Carlo simulation in frequency-selective fading channels and compared to a conventional single carrier system with smart antennas.

This paper is organized as follows. In Section II, the system model of SBM/OFDM is introduced. Section III provides analytical expressions for optimal antenna weights of SBM in a multicarrier system. Section IV considers the issues of multiple-access and proposes an iterative algorithm for ensuring the stability of the network and power optimization. Comparative simulation results are presented in Section V, and finally, we have some concluding remarks in Section VI.

II. SBM/OFDM System Model

The modem configuration of SBM/OFDM is shown in Fig. 1. A serial-to-parallel buffer segments an N_f information bit sequence into N_c parallel output streams. In general, each stream can contain a different number of bits m_c so that

$$N_f = \sum_{c=1}^{N_c} m_c. \tag{1}$$

Paper approved by Y. Li, the Editor for Wireless Communication Theory of the IEEE Communications Society. Manuscript received April 27, 1999; revised January 6, 2000. This work was supported in part by the Hong Kong Telecom Institute of Information Technology. This paper was presented in part at the IEEE GLOBECOM Conference, Sydney, Australia, November 1998.

The authors are with the Center for Wireless Information Technology, Department of Electrical and Electronic Engineering, Hong Kong University of Science and Technology, Clear Water Bay, Hong Kong (e-mail: eewkkit@ee.ust.hk; eecheng@ee.ust.hk; eekhaled@ee.ust.hk; eermurch@ee.ust.hk).

Publisher Item Identifier S 0090-6778(01)00266-5.

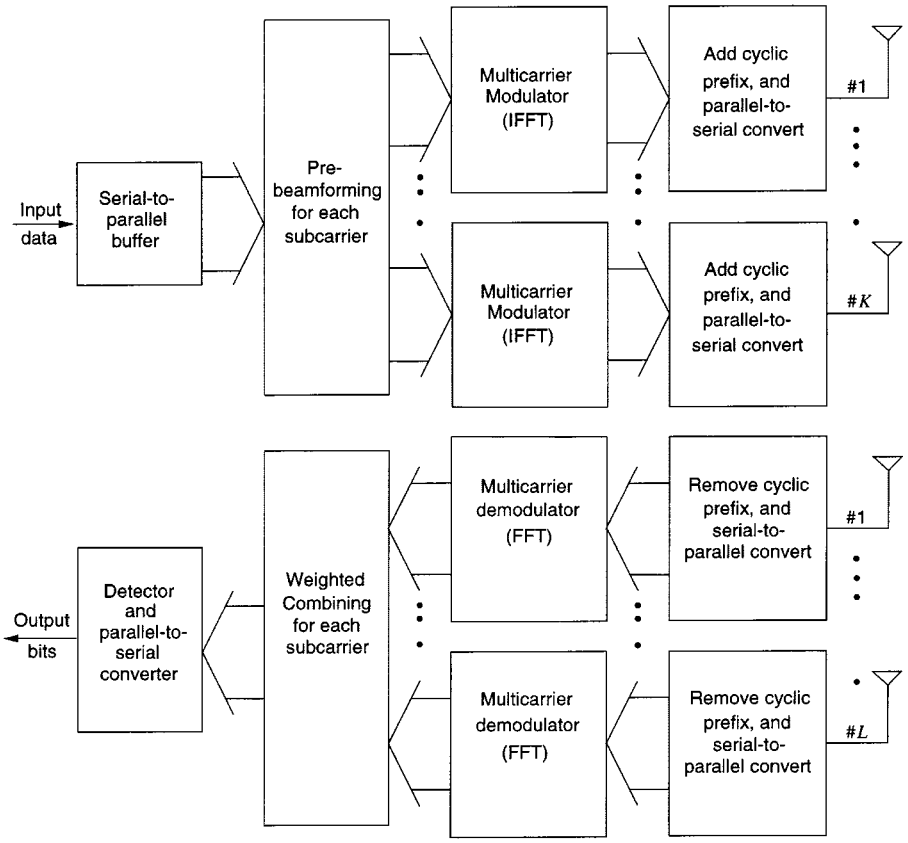

Fig. 1. System configuration of SBM/OFDM.

Each stream can be independently encoded/interleaved, and be regarded as a symbol and mapped into one of 2^{m_c} constellation points. Beamforming with K antenna weights (see next paragraph for details) is then performed, so that K parallel sets of N_c streams are formed. These bit streams are modulated with different subcarriers by passing through an inverse fast Fourier transform (IFFT) processor. A cyclic prefix which is set to the excess delay of the radio channel is also added to each of the resulting signals to reduce the effect of intersubcarrier interference. The bit streams are then converted from parallel-to-serial for final transmission.

The detailed configuration of the beamforming module is shown in Fig. 2(a) where K antennas are located at the BS and the cth subcarrier signal transmitted by the kth antenna is multiplied by a controllable complex weight a_k^c. For convenience, we write the antenna weights at the BS as a vector, so that

$$\mathbf{a}_c = [a_1^c a_2^c \cdots a_K^c]^T \tag{2}$$

where the superscript T denotes the transpose operation.

In total, this implies that there would be $N_c \times K$ weights with the corresponding suggestion that a heavy computation load would be required as compared to a single carrier system. However, several possibilities exist for reducing this load. For example, by exploiting the correlation between adjacent subcarrier channels, it is possible to use the same weight for a number of subcarriers, thereby, reducing the overall computation (see Section V-B for further discussions).

At the receiver side, the cyclic prefix of each received signal is removed, then the subcarrier signals are passed to the fast Fourier transform (FFT) processor, as shown in Fig. 1. The output symbols from the different antennas are weighted and combined to maximize the signal-to-interference-plus-noise ratio (SINR) of the array output signal. The transmitted data are estimated from the combined symbols, and finally, the detected bits are converted back into serial form.

The detailed configuration of the weighted combining is shown in Fig. 2(b) where there are L antennas and the cth subcarrier signal received by the ℓth antenna is multiplied by a controllable complex weight b_ℓ^c. The weighted signals from all L antennas are summed to form a scalar output $s_{o,c}(n)$, and we write the receiver weights in vector notation as

$$\mathbf{b}_c = [b_1^c b_2^c \cdots b_L^c]^T. \tag{3}$$

The wireless communication channel is here characterized by a multipath fading channel. For a particular channel, the multipath model is represented by its channel impulse response using a N-ray model defined as [13], [14]

$$c_{k,\ell}(t) = \sum_{\hat{n}=0}^{N-1} \beta_{k,\ell}^{\hat{n}}\, \delta\left(t - \tau_{k,\ell}^{\hat{n}}\right) \tag{4}$$

where the subscripts k, ℓ refer to the channel between the kth and ℓth antenna at the BS and MS, respectively, and N is the total number of paths. Likewise, $\beta_{k,\ell}^{\hat{n}}$ and $\tau_{k,\ell}^{\hat{n}}$ are, respectively,

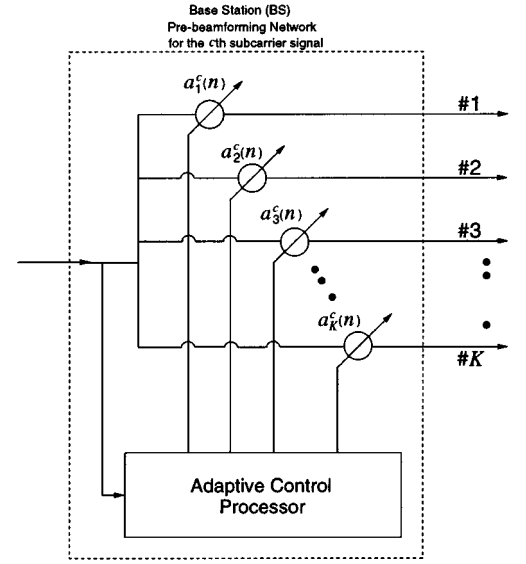

(a)

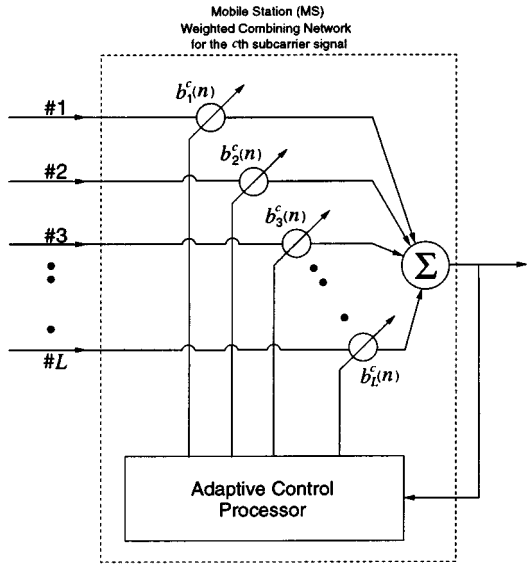

(b)

Fig. 2. System configuration of (a) prebeamforming and (b) weighted combining networks at the BS and MS.

the complex gain and time delay for the $\hat{n}$th path of the diversity channel.

To determine $\beta_{k,\ell}^{\hat{n}}$, we use a statistical approach since it allows easier control of channel parameters such as delay spread. It is assumed that paths with different delays are uncorrelated (i.e., uncorrelated scattering) and that the paths are uncorrelated for each antenna branch so as to provide perfect spatial diversity. As a result, path gains $\beta_{k_1,\ell_1}^{\hat{n}_1}$ and $\beta_{k_2,\ell_2}^{\hat{n}_2}$ are uncorrelated if $k_1 \neq k_2$ or $\ell_1 \neq \ell_2$ or $\hat{n}_1 \neq \hat{n}_2$. In fact, the fading correlation between antennas depends on the angle of arrival, beamwidth and the antenna spacing. In [15], it has been shown that this will be realistic if antenna spacings at the MS and BS are, respectively, greater than 0.4 and 20–40 wavelengths. We refer the readers to [15] for a detailed discussion on the effect of correlation on the antennas. Additionally, the transmitted signals from other users causing CCI are also assumed to suffer from the delay spread of radio channels with uncorrelated path gains. We model $\beta_{k,\ell}^{\hat{n}}$ statistically by zero-mean, complex Gaussian random variables, with their power following the exponential delay profile given by:

$$\mathrm{E}\left[|c_{k,\ell}(t)|^2\right] = \begin{cases} \dfrac{1}{D}\exp(-(t/D)), & \text{for } t \geq 0 \\ 0, & \text{elsewhere} \end{cases} \tag{5}$$

where D is the normalized *root mean square* (rms) delay spread which is defined as the rms delay spread of the channel τ_{rms} divided by the symbol period of transmission T (i.e., $D \triangleq \tau_{\mathrm{rms}}/T$). Although other models of power delay profiles exist, the exponential power profile will be used throughout this paper in order to have a more realistic channel model in analyzing the performance of our proposed systems. In addition, we specifically consider only the paths with delays less than $5D$, so $\tau_{k,\ell}^{\hat{n}} = (5D/(N-1))\,\hat{n}$.

Let $s_c(t)$ denote the transmitted baseband signal at the cth subcarrier frequency, then

$$s_c(t) = \sum_n z_c(n) g(t - nT) \tag{6}$$

where $\{z_c(n)\}$ is the complex symbol sequence at the cth subband and $g(t)$ is the pulse shaping function at the transmitter which gives a band-limited transmit signal. One popular example of $g(t)$ is the raised-cosine pulse shaping filter. In practice, root-raised cosine filters at the transmitter and receiver would be used in order to provide matched filtering when a raised-cosine pulse is implemented.

Let $\mathbf{H}(\hat{n})$ be the channel matrix for the delay time $\hat{n}T$. Hence

$$\mathbf{H}(\hat{n}) = \begin{bmatrix} h_{1,1}(\hat{n}T) & h_{1,2}(\hat{n}T) & \cdots & h_{1,L}(\hat{n}T) \\ h_{2,1}(\hat{n}T) & h_{2,2}(\hat{n}T) & \cdots & h_{2,L}(\hat{n}T) \\ \vdots & & \ddots & \vdots \\ h_{K,1}(\hat{n}T) & \cdots & & h_{K,L}(\hat{n}T) \end{bmatrix} \tag{7}$$

where $h_{k,\ell}(t)$ is equal to $(g \otimes c_{k,\ell} \otimes g)(t)$ in which $c_{k,\ell}(t)$ is defined in (4), and $\otimes$ denotes the convolution operator between two continuous time signals.

Interference is also considered and P interferers are assumed. For now, we consider the downlink only. However, the uplink will be similar. The interfering channel to the ℓth antenna of the desired mobile is defined similar to (4) and the channel vector from the pth interferer at the $\hat{n}T$ delay time sample is

$$\tilde{\mathbf{h}}_p(\hat{n}) = \left[\tilde{h}_{p,1}(\hat{n}T)\tilde{h}_{p,2}(\hat{n}T)\cdots\tilde{h}_{p,L}(\hat{n}T)\right]^T \tag{8}$$

where $\tilde{h}_{p,\ell}(\hat{n}T)$ is the composite channel response from the pth interference to the ℓth antenna of the desired MS link at the $\hat{n}T$ delay.

In this paper, a TDMA-based transmission system is assumed. In particular, data are transmitted in packets over the radio channel and these packets may include a training sequence for synchronization purposes along with information data. In addition, we assume that the channel is quasi-stationary and that it can be considered time-invariant over a packet.

Therefore, the antenna weights for a whole packet of data could be computed through the use of a training sequence.

III. Optimal Antenna Weights

Using the system model described in Section II, our objective here is to find the optimum BS and MS weight vectors $(\mathbf{a}_c, \mathbf{b}_c)$ which maximize the overall SINR at the array output with the constraint of a fixed transmitter power P_T. In the downlink, this is expressed as

$$(\mathbf{a}_c, \mathbf{b}_c)_{\text{opt}} = \underset{\mathbf{b}_c,\, \|\mathbf{a}_c\|^2 = P_T}{\arg\max} \{\text{SINR}\}. \tag{9}$$

Since the analysis will be the same for each subcarrier, it is best to think in terms of a single carrier and then, later, combine together to form a multicarrier system. In our formulation, we assume that the desired channel matrix $\mathbf{H}(\hat{n})$ and the correlation matrix $\mathbf{\Phi}_{u,\,c}$ (will be defined later) are known. In practice, however, we will use pilot tones/symbols to estimate the channel [11], [16] and require the feedback of the estimates.

In a flat fading radio environment, such as a subcarrier of OFDM in a frequency-selective fading radio environment, ISI is negligible. Hence, only the magnitude and phase of the channel at the subcarrier frequency is important. For this reason, we write $\underline{\mathbf{H}}_c$ and $\underline{\tilde{\mathbf{h}}}_{p,\,c}$ as the magnitude and phase of the FFT of $\{\mathbf{H}(\hat{n})\}$ and $\{\tilde{\mathbf{h}}_p(\hat{n})\}$ at the cth subcarrier frequency. Using this notation, the received cth subcarrier signal can be written as

$$\begin{aligned} s_{o,\,c}(n) &= z_c(n)\mathbf{b}_c^H \underline{\mathbf{H}}_c^T \mathbf{a}_c \\ &\quad + \sum_{p=1}^{P} \tilde{z}_{p,\,c}(n)\mathbf{b}_c^H \underline{\tilde{\mathbf{h}}}_{p,\,c} + \mathbf{b}_c^H \mathbf{x}_{n,\,c}(n) \end{aligned} \tag{10}$$

where H denotes the complex conjugate transpose operators, $\mathbf{x}_{n,\,c}(n)$ is a $L\times 1$ column vector with elements modeled as complex additive white Gaussian noise (AWGN) noise with variance of σ_n^2, and $\{\tilde{z}_{p,\,c}(n)\}$ is the transmitted symbol sequence at the cth subcarrier frequency of the pth interfering user, which is uncorrelated with themselves and $\{z_c(n)\}$. In the above equation, the receiver employs perfect timing and the interfering signals are time-aligned with the desired signal (Note that in general the system performance can be sensitive to the time alignment between interfering signals).

The average SINR for the cth subcarrier signal can be written as

$$\Gamma_c = \frac{\sigma_{z_c}^2 \mathbf{b}_c^H \left[\left(\underline{\mathbf{H}}_c^T \mathbf{a}_c\right) \left(\underline{\mathbf{H}}_c^T \mathbf{a}_c\right)^H \right] \mathbf{b}_c}{\mathbf{b}_c^H \mathbf{\Phi}_{u,c} \mathbf{b}_c} \tag{11}$$

where $\mathbf{\Phi}_{u,\,c}$ is the correlation matrix of the undesired signal at the MS at the cth subcarrier frequency, given by

$$\mathbf{\Phi}_{u,\,c} \triangleq \sum_{p=1}^{P} \sigma_{\tilde{z}_{p,\,c}}^2 \underline{\tilde{\mathbf{h}}}_{p,\,c} \underline{\tilde{\mathbf{h}}}_{p,\,c}^H + \sigma_n^2 \mathbf{I} \tag{12}$$

where $\mathbf{I}$ is an identity matrix, and

$$\sigma_{z_c}^2 \triangleq \text{E}\left[|z_c(n)|^2\right] \tag{13}$$

and

$$\sigma_{\tilde{z}_{p,\,c}}^2 \triangleq \text{E}\left[|\tilde{z}_{p,\,c}(n)|^2\right] \tag{14}$$

are defined as the symbol power of the desired user and the pth interfering user at the cth subcarrier frequency, respectively. The matrix (12) can be estimated from

$$\hat{\mathbf{\Phi}}_{u,\,c} = \text{E}[\mathbf{x}\mathbf{x}^H] - \frac{\text{E}[\mathbf{x}r^*]\text{E}[\mathbf{x}r^*]^H}{\sigma_{z_c}^2} \tag{15}$$

during the reference sequence reception period [17], with $\mathbf{x}$ and r being the received signal vector and reference signal, respectively.

By utilizing a standard result in [18], the weight vector $\mathbf{b}_c$ that maximizes the output SINR is

$$\mathbf{b}_c|_{\text{SINR}_{\max}} = \mu \mathbf{\Phi}_{u,\,c}^{-1} \left(\underline{\mathbf{H}}_c^T \mathbf{a}_c\right) \tag{16}$$

where $\mathbf{\Phi}_{u,\,c}^{-1}$ denotes the inverse of $\mathbf{\Phi}_{u,\,c}$, and μ is an arbitrary real constant. In other words, we can find the optimum weights $\mathbf{b}_c$ given that $\mathbf{a}_c$ is known. The difficulty, however, is how to determine the optimum $\mathbf{a}_c$ and the remainder of this section discusses this.

By substituting (16) into (11), it follows that the SINR for a given $\mathbf{a}_c$ can be written as

$$\Gamma_c = \sigma_{z_c}^2 \mathbf{a}_c^H \left[\underline{\mathbf{H}}_c^* \mathbf{\Phi}_{u,\,c}^{-1} \underline{\mathbf{H}}_c^T\right] \mathbf{a}_c. \tag{17}$$

In general, $\mathbf{\Phi}_{u,\,c}$ is a Hermitian and invertible matrix. Thus, $\mathbf{\Phi}_{u,\,c}^{-1}$ is also a Hermitian matrix as is $\mathbf{\Theta}_c \triangleq \underline{\mathbf{H}}_c^* \mathbf{\Phi}_{u,\,c}^{-1} \underline{\mathbf{H}}_c^T$. As a result, it follows that $\mathbf{\Theta}_c$ can be decomposed into

$$\mathbf{\Theta}_c = \mathbf{U}_c \mathbf{\Lambda}_c \mathbf{U}_c^H \tag{18}$$

where $\mathbf{U}_c$ is an unitary matrix whose columns are the eigenvectors of $\mathbf{\Theta}_c$ and $\mathbf{\Lambda}_c$ is a diagonal matrix that contains the corresponding eigenvalues. Consequently

$$\begin{aligned} \Gamma_c &= \sigma_{z_c}^2 \left(\mathbf{U}_c^H \mathbf{a}_c\right)^H \mathbf{\Lambda}_c \left(\mathbf{U}_c^H \mathbf{a}_c\right) = \sigma_{z_c}^2 \acute{\mathbf{a}}_c^H \mathbf{\Lambda}_c \acute{\mathbf{a}}_c \\ &= \sigma_{z_c}^2 \left[\lambda_{c,\,1}|\acute{a}_{c,\,1}|^2 + \lambda_{c,\,2}|\acute{a}_{c,\,2}|^2 + \cdots + \lambda_{K,\,c}|\acute{a}_{c,\,K}|^2\right] \end{aligned} \tag{19}$$

where $\acute{\mathbf{a}}_c$ is defined as $\mathbf{U}_c^H \mathbf{a}_c$ and $\{\lambda_{c,\,k}\}_{k=1}^K$ are the eigenvalues of $\mathbf{\Theta}_c$. Our constant transmitted power constraint, $\|\mathbf{a}_c\|^2 = P_T$ then becomes

$$\begin{aligned} \|\acute{\mathbf{a}}_c\|^2 &= \acute{\mathbf{a}}_c^H \acute{\mathbf{a}}_c \triangleq \left(\mathbf{U}_c^H \mathbf{a}_c\right)^H \left(\mathbf{U}_c^H \mathbf{a}_c\right) \\ &= \mathbf{a}_c^H \mathbf{U}_c \mathbf{U}_c^H \mathbf{a}_c = \mathbf{a}_c^H \mathbf{a}_c = P_T \end{aligned} \tag{20}$$

since $\mathbf{U}_c$ is an unitary matrix. Maximizing the SINR (19) can then be easily performed. Specifically, the optimum weight vector $\acute{\mathbf{a}}_c$ can be shown to be given by [19]

$$\acute{\mathbf{a}}_c|_{\text{SINR}_{\max}} = \sqrt{P_T}[0 \cdots 0 \underbrace{1}_{\text{the } \kappa\text{th element}} 0 \cdots 0]^T \tag{21}$$

where

$$\kappa = \underset{k=1,\,\ldots,\,K}{\arg\max} \{\lambda_{c,\,k}\} \tag{22}$$

and hence we find

$$\mathbf{a}_c = \mathbf{U}_c \acute{\mathbf{a}}_c = \sqrt{P_T}\mathbf{v}(\mathbf{\Theta}_c) \tag{23}$$

where $\mathbf{v}(\mathbf{\Theta}_c)$ is the eigenvector of the matrix $\mathbf{\Theta}$ that corresponds to the largest eigenvalue. Throughout, we will refer to

$\mathbf{v}(\mathbf{\Theta}_c)$ as the largest eigenvector of the matrix $\mathbf{\Theta}_c$. As a consequence, the corresponding maximum SINR at the cth subcarrier frequency is given by

$$\begin{aligned}\Gamma_c &= \sigma_{z,c}^2 \mathbf{a}_c^H \mathbf{\Theta}_c \mathbf{a}_c \\ &= \sigma_{z,c}^2 \left(\sqrt{P_T}\mathbf{v}(\mathbf{\Theta}_c)\right)^H \mathbf{\Theta}_c \left(\sqrt{P_T}\mathbf{v}(\mathbf{\Theta}_c)\right) \\ &= \sigma_{z,c}^2 P_T \lambda_{c,\kappa} \end{aligned} \tag{24}$$

where $\lambda_{c,\kappa}$ is the largest eigenvalue of the matrix $\mathbf{\Theta}_c$. Therefore, the maximum SINR we can achieve with the constraint $||\mathbf{a}_c||^2 = P_T$ is given by (24), and is achieved when the weight vectors (16) and (23) are used.

It should be noted that in order to compute the transmit weights at a particular subcarrier, the number of multiplications required is $(K^2 + L^2)(K + L)$. Therefore, the computational requirement would be quite involved when K or L is large. However, algorithms like Lagrange algorithm and many variants exist to reduce the computation load of eigenvalue decomposition (EVD). Hence, in practice, the hardware requirement can be simplier.

IV. Multiple Access

In OFDM systems, multiple users or multiple access can be provided by using different time slots on the subcarriers. By incorporating smart antennas at both the BS and MS, it is expected that extra users can be supported and we refer to this multiple-access technique as *spatial subcarrier multiple access* (SSCMA). In multiple-access environments, there will be more than one MS and BS. Hence, it is important that we try and determine the stability of SBM under these conditions.

Stability is an issue because the adjustment of the antenna weights at a particular BS transmitter for improving the link quality of its target MS receiver will also interfere with other users. Consequently, other users would try to counteract the problem of readjustment of their antenna weights and the overall wireless network may become unstable. Here, we present an iterative approach for the adjustment of the weights.

In general, there will be Q MSs with which $\underline{P}$ BSs communicate. To cope with this, we invoke some additional notation. We denote the BS weight and correlation matrix for MS q as $\mathbf{a}_{q,c}$ and $\mathbf{\Phi}_{u_q,c}$, respectively, for the cth subchannel. Similarly, we denote the cth downlink subchannel between the qth MS and the BS that communicates with the $\tilde{q}$th MS as $\underline{\mathbf{H}}_{b_{\tilde{q}},q,c}$. Using this notation, we can describe our iterative process as follows, where superscript (i) is used to denote the ith iteration.

- Step 1) For all MSs, initialize $\mathbf{a}_{q,c}^{(i=0)}$ by

$$\mathbf{a}_{q,c}^{(i=0)} = \sqrt{P_T}\mathbf{v}\left(\underline{\mathbf{H}}_{b_q,q,c}^* \underline{\mathbf{H}}_{b_q,q,c}^T\right). \tag{25}$$

- Step 2) $i = i + 1$

$$\begin{aligned}\mathbf{\Phi}_{u_q,c}^{(i)} = &\sum_{\tilde{q}\neq q} \sigma_{\tilde{q},c}^2 \left(\underline{\mathbf{H}}_{b_{\tilde{q}},q,c}^T \mathbf{a}_{\tilde{q},c}^{(i-1)}\right) \\ &\cdot \left(\underline{\mathbf{H}}_{b_{\tilde{q}},q,c}^T \mathbf{a}_{\tilde{q},c}^{(i-1)} v\right)^H + \sigma_n^2 \mathbf{I} \end{aligned} \tag{26}$$

and compute

$$\mathbf{a}_{q,c}^{(i)} = \sqrt{P_T}\mathbf{v}\left(\underline{\mathbf{H}}_{b_q,q,c}^* \mathbf{\Phi}_{u_q,c^{(i)}}{}^{-1} \underline{\mathbf{H}}_{b_q,q,c}^T\right) \tag{27}$$

for all Q MSs.

- Step 3) Repeat Step 2) until convergence.

The process intends to balance the SINRs for all the links and at convergence, the minimum SINR of all the links will be maximized.

In some situations, a more suitable requirement would be for each link to meet a specific SINR Γ_o. To perform this, we initially preset the power allocated and use the algorithm described above to find the optimum weights. We then perform power allocation using

$$\sigma_{q,c}^{(i)^2} = \frac{\Gamma_o}{\Gamma_{q,c}^{(i-1)}} \sigma_{q,c}^{(i-1)^2} \tag{28}$$

where $\sigma_{q,c}^2$ and $\Gamma_{q,c}$ denote the power allocated by and SINR for the qth MS at the cth subchannel, respectively [the SINR $\Gamma_{q,c}$ can be calculated by (24)]. The optimum weights for this power allocation, using (25)–(27), are then obtained, after which power allocation using (28) is performed again. This is continued until convergence.

For each iteration, the process tries to solve the joint optimal weights at the BS and MS while treating the CCI fixed, so the objective function changes from iteration to iteration. In fact, this multiobjective optimization problem is not convex and highly nonlinear [20]. As such, there is no guarantee that the method will converge and obtain the joint optimal weights for each user. However, we have performed extensive computer simulation over various operating conditions and have experienced no instability problem.

V. Simulation Results

The SBM/OFDM system introduced in Section II is investigated for a TDMA/TDD-based wireless communication system by computer simulation. All channel state information is estimated using pilot tones. The configurations considered are for OFDM systems with a 5-MHz transmission bandwidth, 1024 subcarriers, and various numbers of antennas at the BS and MS. For each technique, simulations of average error probability (P_e) are provided for various CCI [signal-to-interference ratio (SIR)] and AWGN (SNR). The results are compared with a *conventional* adaptive antenna system where smart antennas are used at the BS only. Results for SBM using a single carrier are also listed for comparison.

To refer to the different antenna configurations, we use the notation $K + L$. For example, when we use SBM and OFDM with three antennas at BS and two antennas at MS, we refer to it as *3 + 2 SBM/OFDM*. For a conventional adaptive antenna system with two antennas at the BS only and a single carrier, we write it as *2 + 1*. For a conventional OFDM system, we write it as *2 + 1 Conv/OFDM*.

For each P_e simulation, data packets consisting of 1000 data symbols are transmitted with more than 5000 independent channels [21]. For the transmitted signals, a root-raised cosine pulse

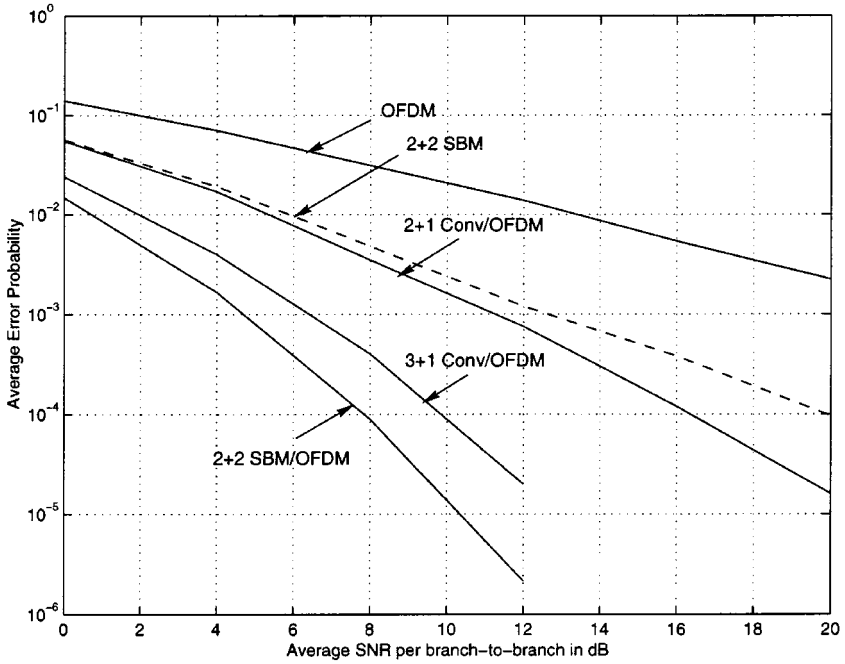

Fig. 3. Average bit-error probability performance of $2 + 2$ SBM/OFDM in multipath fading channels in the absence of CCI.

shaping filter with rolloff factor of 0.22 is used. In the simulation, we utilize frequency-selective Rayleigh fading channels which can be characterized by the normalized delay spread D (defined in Section II). The parameter D is an important and convenient measure of the degree of the frequency selectivity of the channel. In particular, in digital transmission over multipath channels, the BER is highly dependent on D [1].

In our simulation, for multicarrier modulation, we use a symbol period T of 0.2 ms, and a delay spread $\tau_{\rm rms}$ of 100 ns. For SBM without frequency-division multiplexing, the symbol period is $T/1024 = 195$ ns in order to achieve the same throughput as that of multicarrier transmission. The rms delay spread normalized by the symbol period in this case is then 0.512. For the single carrier system, simulations are done at this value of D for comparison. Finally, the channel of each link contains ten random multipath components [$N = 10$ in (4)] with $\tau_{\rm rms} = 100$ ns.

A. SBM/OFDM in Frequency-Selective Fading

In Fig. 3, we provide results for the configurations of $2 + 1$ Conv/OFDM, $3 + 1$ Conv/OFDM, $2 + 2$ SBM, and $2 + 2$ SBM/OFDM, all with QPSK modulation, over frequency-selective fading channels. A close observation of Fig. 3 reveals that more than a tenfold reduction in P_e is possible for $2 + 2$ SBM compared with OFDM without smart antennas. However, the performance of $2 + 1$ Conv/OFDM and $3 + 1$ Conv/OFDM is much better than that of SBM without OFDM. This implies that combined smart antennas and multicarrier modulation can have significant improvement in system performance and for $2 + 2$ SBM/OFDM, a more than 1000-fold decrease in P_e performance compared to OFDM occurs. Additionally, it is also about 2 dB more power efficient than $3 + 1$ Conv/OFDM. It should also be noted that the results of SBM/OFDM are similar to that of SBM in flat fading channels (see [11]).

In Fig. 4, results for the same configurations as in Fig. 3 are provided but for a single CCI of SIR $= 15$ dB. Results illustrate that $2 + 2$ SBM/OFDM is consistently 2 dB better than $3 + 1$ Conv/OFDM and has about a 100 times reduction in average error performance compared to $2 + 1$ Conv/OFDM or $2 + 2$ SBM.

It is also important to note that for both SBM and SBM/OFDM, channel information is required. When the channel is frequency-nonselective, closed-form solution of antenna weights (Section III) can be used to obtain smart antennas at both BS and MS. However, for SBM in frequency-selective fading channels, a more computationally extensive iterative process is required [11]. This not only increases the complexity of the signal processing, but also results in worse performance compared with that in flat fading channels when compared to SBM/OFDM.

B. Complexity Reduction

In Section III, the joint antenna weights at the BS and MS are derived for SINR maximization. It is noted that the calculation of the antenna weights in (23) for every subcarrier requires an EVD as well as matrix inversion. This could imply an enormous computation burden when K or L is large. However, the fact that adjacent subcarriers can be correlated (depending on the coherence bandwidth), reduction in complexity is possible.

Consider an OFDM system with transmission bandwidth of 5 MHz and 1024 subcarriers. Then, the subcarrier bandwidth is given by

$$\Delta f = \frac{5 \times 10^6}{1024} = 4.88\,\text{kHz}. \tag{29}$$

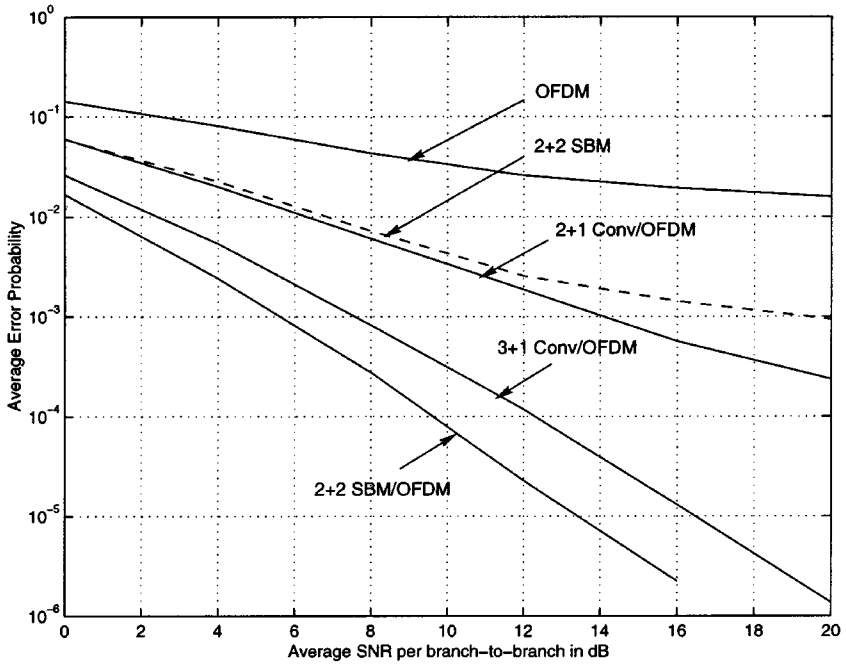

Fig. 4. Average bit-error probability performance of $2 + 2$ SBM/OFDM in multipath fading channels under the condition of single CCI at SIR $= 15$ dB.

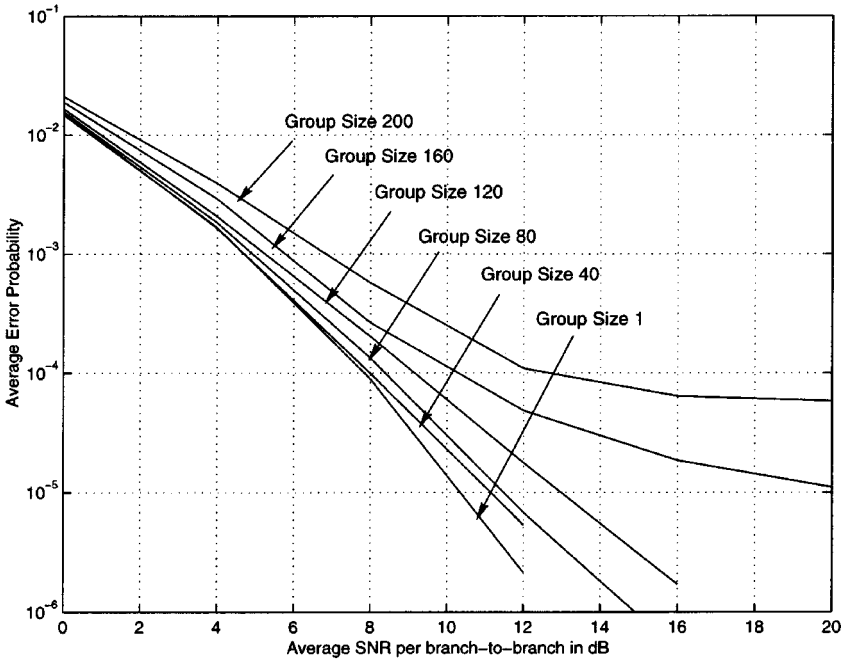

Fig. 5. Average bit-error probability performance of $2 + 2$ SBM/OFDM with different group size in the absence of CCI.

Assume that the rms delay spread, $\tau_{\rm rms}$ is 100 ns, then the coherence bandwidth for a frequency correlation greater than 0.9 is approximately

$$BW_c \approx \frac{1}{50\tau_{\rm rms}} = 0.2\,\text{MHz} \approx 40\Delta f. \tag{30}$$

As a result, about 40 consecutive subcarriers are faded coherently. This implies that it is possible to use the same set of antenna weights for a number of subcarriers instead of calculating smart antenna weights for every individual subcarrier. Using this approach, the computational complexity can be reduced significantly. In fact, such complexity can be further reduced with only a little degradation in performance, by allowing less correlated frequency subcarriers to share the same antenna weights.

To demonstrate this, simulation results, as illustrated in Fig. 5, are provided for $2 + 2$ SBM/OFDM with QPSK in the absence of CCI, using the same antenna weights for a group of subcarriers. Group sizes of 1, 40, 80, 120, 160, and 200 are considered.

Results show that there is less than 1-dB P_e performance degradation for group size of 40 compared with calculating the weights for every subcarrier (i.e., group size equals 1).

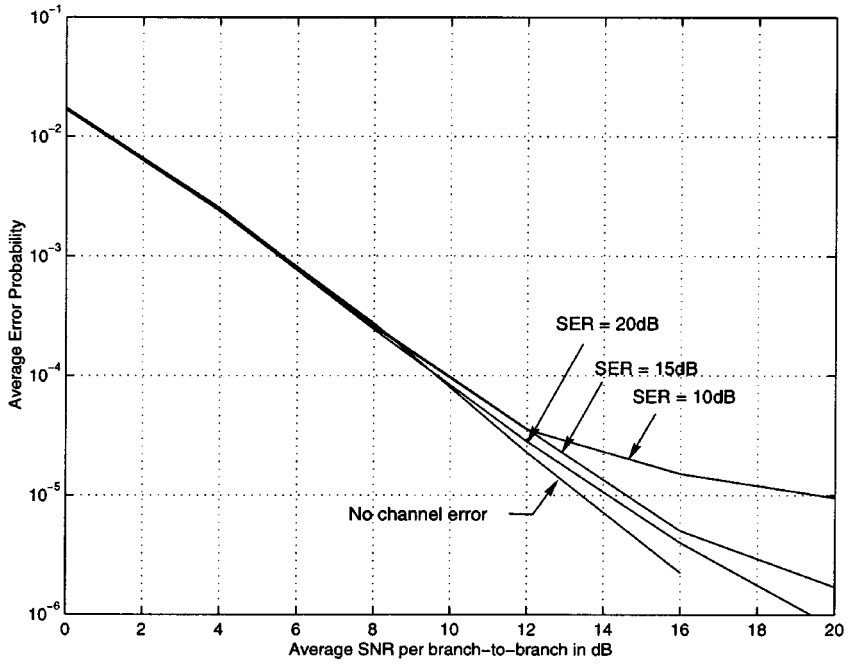

Fig. 6. Average bit-error probability performance of $2 + 2$ SBM/OFDM in multipath fading channels under the condition of single CCI at SIR $= 15$ dB in the presence of channel estimation errors.

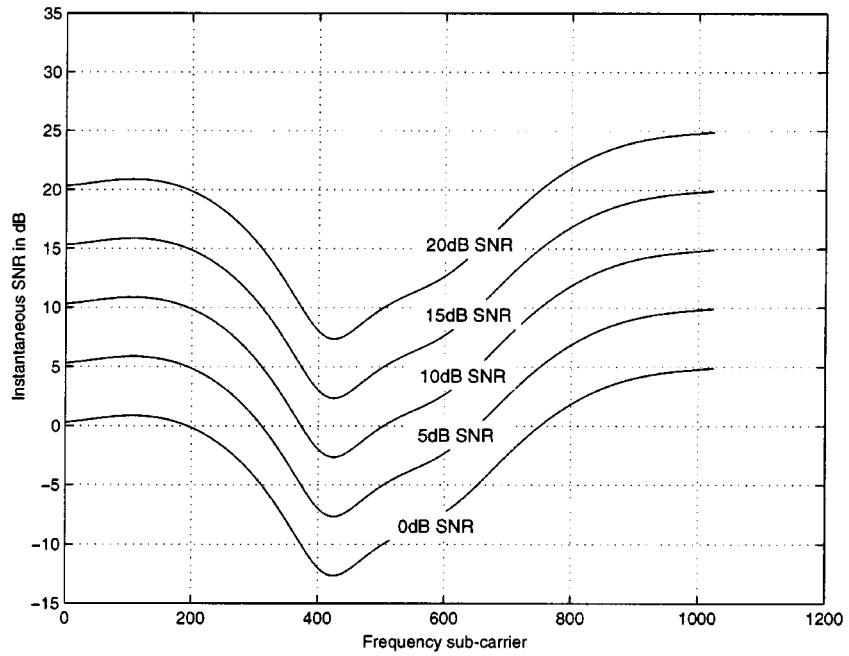

Fig. 7. Variations of instantaneous SNR values for all frequency subcarriers of an OFDM system without antenna diversity in the absence of CCI.

However, it is possible to further reduce the computational complexity with very little performance degradation. A group size of 80 seems the best choice where an 80 times reduction in computational complexity can be achieved with very little P_e performance degradation. In addition, group sizes of 120, 160, or 200 are provided and less than 10^{-4} P_e can also be achieved. Therefore, it is possible to have even lower computational complexity to implement SBM/OFDM when a higher P_e is tolerable.

C. Sensitivity to Channel Errors

As discussed previously, channel information must be estimated, and some feedback from the receiver is required, when carrying out SBM/OFDM. In real situations, this information might have some errors depending on the channel quality as well as the ability of the channel estimation method used. In order to estimate the system performance of SBM/OFDM in a more realistic way, the P_e performance of SBM/OFDM in which the channel and feedback information are in errors is investigated.

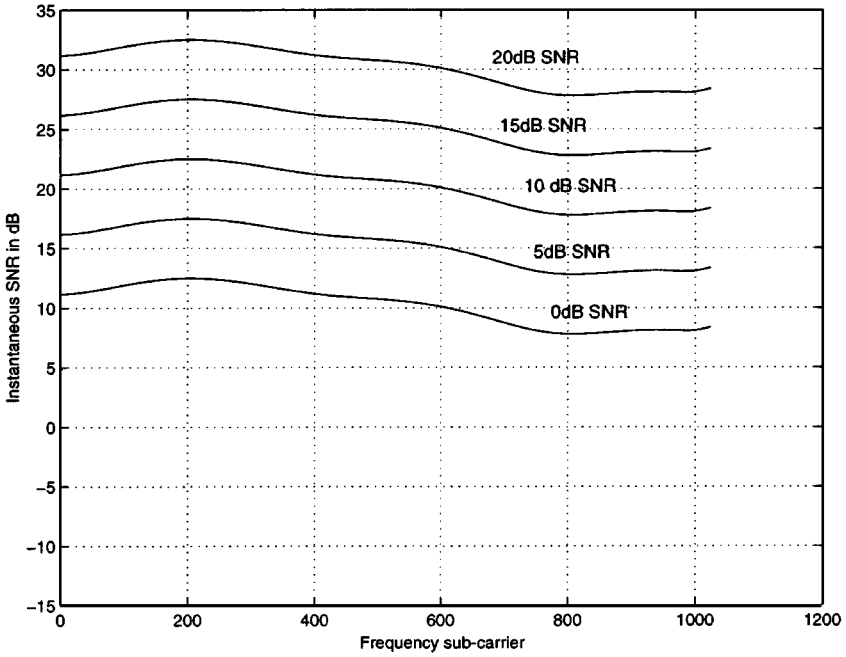

Fig. 8. Variations of instantaneous SNR values for all frequency subcarriers of $2 + 2$ SBM/OFDM in the absence of CCI.

To study the sensitivity of our system to channel errors, we model the estimation error e as zero-mean complex AWGN with variance σ_e^2, so that

$$\hat{h}^c_{k,\ell} = h^c_{k,\ell} + e_{k,\ell}, \qquad \text{for } k = 1, \ldots, K;\ \ell = 1, \ldots, L \tag{31}$$

$$\hat{\phi}^c_{m,n} = \phi^c_{m,n} + e_{m,n}, \qquad \text{for } m, n = 1, \ldots, K \tag{32}$$

where $\hat{h}^c_{k,\ell}$ and $\hat{\phi}^c_{m,n}$ are the estimates of $h^c_{k,\ell}$ (elements of $\underline{\mathbf{H}}_c$) and $\phi^c_{m,n}$ (elements of $\mathbf{\Phi}_{u,c}$), respectively. To characterize the errors, we define the term, signal-to-error ratio (SER), which is given by $|h^c_{k,\ell}|^2/\sigma_e^2$ or $|\phi_{m,n}|^2/\sigma_e^2$.

In Fig. 6, results are provided for multipath fading channels in the presence of CCI with $\mathrm{SIR} = 15$ dB for $\mathrm{SER} = 10, 15, 20, \infty$ dB. Note that in noise-limited scenarios (i.e., less than 15 dB), the performance is not sensitive to channel estimation errors and has extremely little degradation. On the other hand, in interference limited environments, accurate channel estimation becomes important.

D. Channel Variation Among Subcarriers

In OFDM systems, improved performance can be achieved by power allocation and adaptive modulation [22]. Application of power allocation and adaptive modulation may also be of benefit to smart antenna systems using OFDM. Raleigh and Cioffi [8] have studied the capacity of a multiple-input (transmit antenna) and multiple-output (receive antenna) (MIMO) systems. Results reveal that in MIMO/OFDM systems, parallel spatial subchannels can be created for every subcarrier. Power allocation and adaptive modulation [22] can then be applied to every parallel spatial subcarrier to improve the capacity and/or performance. However, this approach cannot be used easily in the presence of CCI as the antenna weights at the receiver are needed to suppress CCI rather than create parallel spatial subchannels.

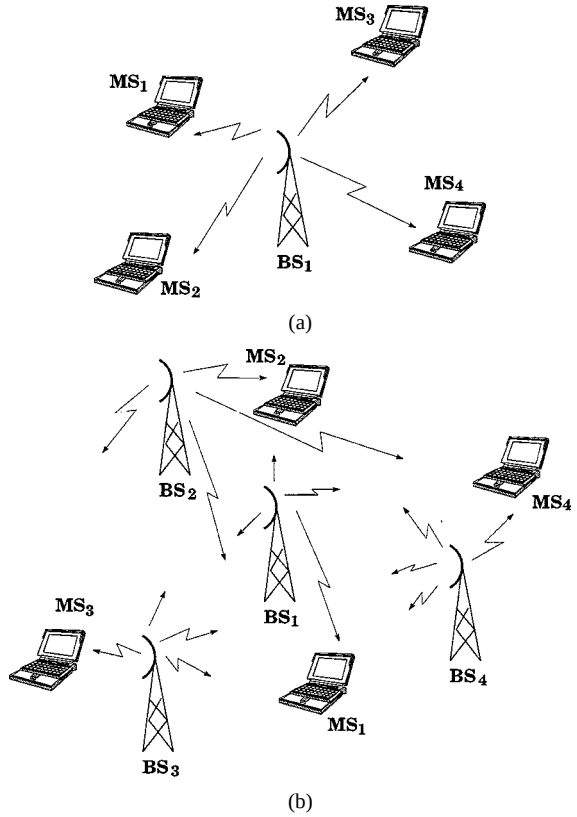

Fig. 9. Examples when (a) $b_1 = b_2$ and (b) $b_1 \neq b_2$.

Here, we will demonstrate by simulation results that the need for adaptive bit and power allocation is significantly reduced by the joint smart antennas at the BS and MS. In Figs. 7 and 8, results are provided for OFDM and $2 + 2$ SBM/OFDM using QPSK modulation, respectively, in the absence of CCI. Since

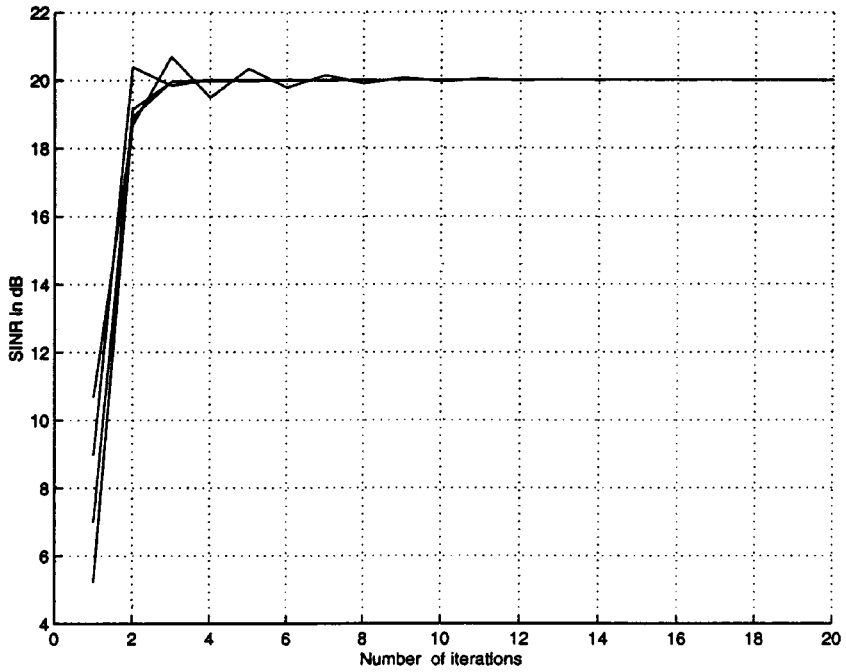

Fig. 10. Convergence of SINR for all the links for Example 1 ($4 + 4$ SBM/OFDM, $Q = 4$ and $\Gamma_o = 20$ dB).

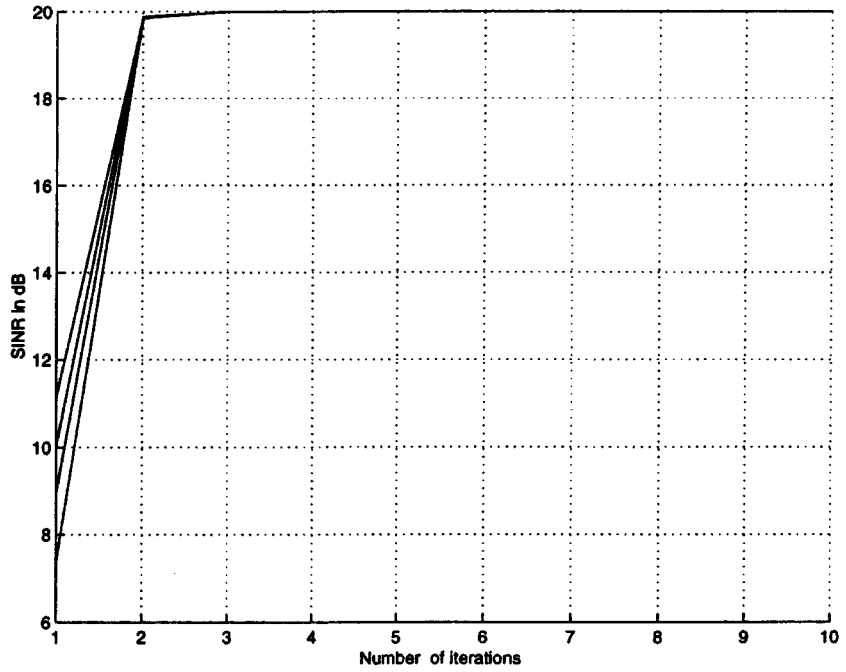

Fig. 11. Convergence of SINR for all the links for Example 2 ($4 + 4$ SBM/OFDM, $Q = 4$ and $\Gamma_o = 20$ dB).

the bit-error probability performance is highly dependent on the SNR, SNR performance for all subcarriers are provided to view the channel variations.

A close observation of Fig. 7 illustrates that for OFDM without antenna diversity, deep fades are evident and up to 15 dB variation in SNR can occur. As a result, it is expected that adaptive bit and power allocation would be extremely useful since most of the faded subcarriers would be unused. In contrast, Fig. 8 shows that for $2 + 2$ SBM/OFDM, the channel variation (i.e., SINR) is less (3 dB variation) compared to OFDM without antenna diversity. As a result, fading is reduced by the smart antennas and therefore, the need for adaptive bit and power allocation is reduced. Results have also been obtained, under the condition of a single CCI at SIR $=$ 15 dB. These indicate a similar trend, in which the fades are successfully alleviated by the antennas.

E. Multiuser SBM/OFDM

As discussed in Section IV, it is important to determine the stability of SBM/OFDM in multiple-access environments in which the transmit weighted combining and power allocation for every user must be controlled jointly to ensure the stability

of the networks. Here, we describe two examples Fig. 9 that demonstrate stability. In Fig. 9(a), a space-division multiple-access (SDMA) environment is considered, where more than one user is communicating within the same frequency-time channel in the same cell. While in Fig. 9(b), multiple users are shared with the same frequency-time channel only when they are in a different cell (i.e., a conventional FDMA system using frequency reuse).

Example 1: As illustrated in Fig. 9(a), four users are communicating with one BS in the same traffic channel simultaneously. Using $4 + 4$ SBM/OFDM for all four users, we have plotted the transient results of the SINR for each user in Fig. 10. Using the algorithm detailed in Section IV, the x-axis represents the number of iterations of (28) while the number of iterations of (25)–(27) is set to 5 for achieving convergence. In the simulation, the target SINR Γ_o is set to 20 dB for all users.

Results reveal that 12 iterations are required to achieve absolute convergence and the average required transmit power above noise is only 13 dB. At convergence, the transmit powers for all users are minimized while ensuring SINR $=$ 20 dB for all users.

Example 2: Users 1–4 are communicating with BSs $b_1 - b_4$, respectively, in the same traffic channel, as shown in Fig. 9(b). For the same setup as that of Example 1 (i.e., $K = 4$, $L = 4$, $Q = 4$, and $\Gamma_o = 20$ dB), but with an average SIR $= 15$ dB at each cell, the transient property of SINR for all the users is plotted in Fig. 11 using the algorithm detailed in Section IV. From Fig. 11, we note that after three iterations, we achieve convergence. Results also reveal that when the system is operating in steady state, the SIR increases from 15 to 20 dB (reaching our target Γ_o), and the average required transmit power above noise is 11 dB.

In general, the iterative process described in Section IV appears to converge for an MIMO system with $Q \leq \min(K, L)$ and the steady-state performance improves the intercell and intracell SINR (or minimizes transmit power for each user while guaranteeing $\mathrm{SINR} \geq \Gamma_o$). As a consequence, the same traffic channel can be reused more frequently to increase the system capacity.

VI. Conclusions

This paper has demonstrated that the combination of OFDM with smart antennas provides improvements in performance compared to wireless communication systems based on OFDM or smart antennas alone. Simulation results show that our system can reduce the average error probability by more than 1000 times for frequency-selective fading channels, as compared to OFDM without antenna diversity. Also, the required transmit power for each user is minimized while maintaining guaranteed quality of service for each user. In this multiuser SBM/OFDM system, users are able to be separated by time and/or frequency subcarrier, as well as space. Thereby, enhancing the system capacity and reducing the power consumption of transmission significantly.

The implementation of the system, however, requires that multiple antennas be incorporated into the base, and mobile as well. As a consequence, we suggest its suitability for wireless LAN applications in combination with recent advances in compact antenna design.

Acknowledgment

The authors would like to thank the anonymous reviewers for their very useful and constructive comments.

References

[1] K. B. Letaief, J. C.-I. Chuang, and R. D. Murch, "A high-speed transmission method for wireless personal communications," in *Wireless Personal Communications.* Norwell, MA: Kluwer, 1996, pp. 299–317.

[2] C. G. Günther, J. E. Padgett, and T. Hattori, "Overview of wireless personal communications," *IEEE Commun. Mag.*, vol. 33, pp. 28–41, Jan. 1995.

[3] V. Tarokh, N. Seshadri, and A. R. Calderbank, "Space-time codes for high data rate wireless communications: Performance criterion and code construction," *IEEE Trans. Inform. Theory*, vol. 44, pp. 744–765, Mar. 1998.

[4] Y. Chen, K. B. Letaief, and J. C.-I. Chuang, "Soft-output equalization and TCM for wireless personal communications systems," *IEEE J. Select. Areas Commun.*, vol. 16, pp. 1679–1690, Dec. 1998.

[5] J. H. Winters, "Signal acquisition and tracking with adaptive arrays in the digital mobile radio system IS-54 with flat fading," *IEEE Trans. Veh. Technol.*, vol. 42, pp. 377–384, Nov. 1993.

[6] J. Fuhl and A. F. Molisch, "Capacity enhancement and BER in a combined SDMA/TDMA system," in *Proc. IEEE VTC'96*, vol. 3, New York, 1996, pp. 1481–1485.

[7] C. R. Rowell and R. D. Murch, "A capacitively loaded PIFA for compact mobile telephone handsets," *IEEE Trans. Antennas Propagat.*, vol. 45, pp. 837–842, May 1997.

[8] G. G. Raleigh and J. M. Cioffi, "Spatio-temporal coding for wireless communications," in *Proc. IEEE Globecom'96*, London, U.K., Nov. 1996, pp. 1809–1814.

[9] R. Kohno, "Spatial and temporal communication theory using software antennas for wireless communications," in *Proc. PIMRC'97*, Helsinki, Finland, Sept. 1–4, 1997, pp. 293–321.

[10] I.-T. Lu and J.-S. Choi, "Space-time processing for broadband multi-channel communication systems using smart antennas at both transmitter and receiver," in *Proc. IEEE ICC'99*, vol. 1, Vancouver, BC, Canada, Jan. 6–10, 1999, pp. 1–5.

[11] K.-K. Wong, K. B. Letaief, and R. D. Murch, "Investigating the performance of smart antenna system at the mobile and base stations in the down and uplinks," in *Proc. IEEE VTC'98*, vol. 2, Ottawa, ON, Canada, May 18–21, 1998, pp. 880–884.

[12] J. A. C. Bingham, "Multicarrier modulation for data transmission: An idea whose time has come," *IEEE Commun. Mag.*, pp. 5–14, 1990.

[13] L. F. Chang and J. C.-I. Chuang, "Diversity selection using coding in a portable radio communications channel with frequency-selective fading," *IEEE J. Select. Areas Commun.*, vol. 7, pp. 89–97, Jan. 1989.

[14] K. B. Letaief, K. Muhammad, and J. S. Sadowsky, "Fast simulation of DS/CDMA with and without coding in multipath fading channels," *IEEE J. Select. Areas Commun.*, vol. 15, pp. 626–639, May 1997.

[15] J. Salz and J. H. Winters, "Effect of fading correlation on adaptive arrays in digital mobile radio," *IEEE Trans. Veh. Technol.*, vol. 43, pp. 1049–1057, Nov. 1994.

[16] J. K. Cavers, "An analysis of pilot assisted modulation for Rayleigh fading channels," *IEEE Trans. Veh. Technol.*, vol. 40, pp. 686–693, Nov. 1991.

[17] K. Yokohata, Y. Ogawa, and K. Itoh, "Spatial-domain path diversity using an adaptive array for mobile communications," in *Proc. IEEE ICUPC'95*, 1995, pp. 600–604.

[18] J. R. T. Comption, *Adaptive Antennas Concepts and Performance*. Englewood Cliffs, NJ: Prentice-Hall, 1988.

[19] *Linear Algebra and Its Application*. San Diego, CA: Harcourt Brace Jovanovich, 1988.

[20] K.-K. Wong, R. S.-K. Cheng, K. B. Letaief, and R. D. Murch, "Optimizing the spectral efficiency of multiuser MIMO smart antenna systems," in *Proc. IEEE WCNC*, Chicago, IL, Sept. 2000.

[21] J. C.-L. Ng, K. B. Letaief, and R. D. Murch, "Antenna diversity combining and finite-tap decision feedback equalization for high-speed data transmission," *IEEE J. Select. Areas Commun.*, vol. 16, pp. 1367–1375, Oct. 1998.

[22] D. Hughes-Hartogs, "Ensemble modem structure for imperfect transmission media," U.S. Patent 4 679 227 (July 1987), 4 731 816 (March 1988), and 4 833 796 (May 1989).

Kai-Kit Wong (S'99) was born in Hong Kong in 1973. He received the B.Eng. and M.Phil. degrees in electronic engineering from the Hong Kong University of Science and Technology, Clear Water Bay, Hong Kong, respectively, in 1996 and 1998. He is currently working toward the Ph.D. degree in electrical and electronic engineering also at the Hong Kong University of Science and Technology.

He has worked in several areas including smart antennas, space-time coding and equalization. His current research interest centers around the joint optimization of smart antennas for multiuser wireless communications.

Mr. Wong received a VTS Japan Chapter Award of the VTC2000-Spring in Japan.

Roger S.-K. Cheng (S'86–M'92) received the B.S. degree from Drexel University, Philadelphia, PA, in 1987, and the M.A. and Ph.D. degrees from Princeton University, Princeton, NJ, in 1988 and 1991, respectively, all in electrical engineering.

From 1987 to 1991, he was a Research Assistant in the Department of Electrical Engineering, Princeton University, Princeton, NJ. From 1991 to 1995, he was an Assistant Professor in the Electrical and Computer Engineering Department, University of Colorado at Boulder. In June 1995, he joined the Faculty of the Hong Kong University of Science and Technology, where he is currently an Associate Professor in the Department of Electrical and Electronic Engineering. He has also held visiting positions with Qualcomm, San Diego, CA, in the summer of 1995, and with the Institute for Telecommunication Sciences, NTIA, Boulder, CO, in the summers of 1993 and 1994. His current research interests include wireless communications, OFDM, space–time processing, CDMA, digital implementation of communication systems, wireless multimedia communications, information theory, and coding.

Dr. Cheng is currently an Editor for Wireless Communication for the IEEE TRANSACTIONS ON COMMUNICATIONS. He has served as Guest Editor of the special issue on Multimedia Network Radios in the IEEE JOURNAL ON SELECTED AREAS IN COMMUNICATIONS, Associate Editor of the IEEE TRANSACTION ON SIGNAL PROCESSING, and Membership Chair for of the IEEE Information Theory Society. He is the recipient of the Meitec Junior Fellowship Award from the Meitec Corporation in Japan, the George Van Ness Lothrop Fellowship from the School of Engineering and Applied Science in Princeton University, and the Research Initiation Award from the National Science Foundation.

Khaled Ben Letaief (S'85–M'86–SM'97) received the B.S. degree (with distinction) in electrical engineering and the M.S. and Ph.D. degrees from Purdue University, West Lafayette, IN, in 1984, 1986, and 1990, respectively.

Since January 1985, as a Graduate Instructor in the School of Electrical Engineering at Purdue University, he has taught courses in communications and electronics. From 1990 to September 1993, he was a Member of Academic Staff at the Department of Electrical and Electronic Engineering, University of Melbourne, Melbourne, Australia, where he has been also a Member of the Center for Sensor Signal and Information Systems. Since September 1993, he has been with the Department of Electrical and Electronic Engineering, Hong Kong University of Science and Technology (HKUST), where he is currently an Associate Professor. From 1995 to 1998, he was Director of the the department's undergraduate studies program. His research interests include wireless personal and mobile communications, spread-spectrum systems, optical fiber networks, multiuser detection, wireless multimedia communications, and CDMA systems.

Dr. Letaief has been an active member of various professional societies and has published papers in several journals and conference proceedings. He is an Editor for the *Wireless Personal Communications Journal*, and he served as a Guest Editor for the 1998 *Wireless Personal Communications Journal* special issue on "Intelligent Multimedia Systems, Terminals, and Components." He is also the Editor for Wireless Systems of the IEEE TRANSACTIONS ON COMMUNICATIONS, and a Technical Editor of the IEEE COMMUNICATIONS MAGAZINE. He was a Guest Editor of the 1997 IEEE JOURNAL ON SELECTED AREAS IN COMMUNICATIONS special issue on "Computer-Aided Modeling, Analysis, and Design of Communications Links." In addition, he served as Technical Program Chair of the 1998 IEEE Mini-Conference on Communications Theory (CTMC'98), which was held in Sydney, Australia, November 1998, and Chair of the 2001 IEEE Communications Theory Symposium, held in Helsinki, Finland, June 2001. He is currently an Officer in the IEEE Communications Society Technical Committee on Personal Communications. He received the Mangoon Teaching Award from Purdue University om 1990; the Teaching Excellence Appreciation Award from the School of Engineering, HKUST, in Spring 1995, Fall 1996, Fall 1997, and Spring 1999; and the Michael G. Gale Medal for Distinguished Teaching (highest university teaching award) in 1998.

Ross D. Murch (S'85–M'87–SM'98) received the Ph.D. degree in electrical and electronic engineering from the University of Canterbury, Christchurch, New Zealand, in 1990.

He is an Associate Professor in the Department of Electrical and Electronic Engineering, Hong Kong University of Science and Technology. From August–December 1998, he was on sabbatical leave at Allgon Mobile Communications, Sweden (manufactures approximately 1 000 000 handset antennas per week), and AT&T Research Labs, New Jersey. He is also the founding Director of the Center for Wireless Information Technology, which began in August 1997. He has several U.S. patents related to wireless communication, over 100 published papers and acts as a consultant for industry on occasions. His research interests include MIMO antenna systems and compact antenna design for wireless communications.

Dr. Murch is an Editor for the IEEE JOURNAL OF SELECTED AREAS IN COMMUNICATIONS: WIRELESS SERIES and acts as reviewer for several journals. He is a Chartered Engineer and also an URSI correspondent. He won an URSI Young Scientist and Engineering Teaching Excellence Appreciation Awards in 1993 and 1996, respectively.